Multifunctional Nanoprobes

DOI: 10.1002/ange.200704392

$Au–Fe_3O_4$ Dumbbell Nanoparticles as Dual-Functional Probes**

*Chenjie Xu, Jin Xie, Don Ho, Chao Wang, Nathan Kohler, Edward G. Walsh, Jeffrey R. Morgan, Y. Eugene Chin, and Shouheng Sun**

Synthesis of dumbbell-shaped nanoparticles containing different functionalities has attracted much attention recently.[1] In such a dumbbell structure, one nanoparticle is linked to another, and electronic communication across the junction can drastically change the local electronic structure, leading to an additional dimension of control in catalytic, magnetic, and optical properties.[2] Moreover, the dumbbell structure offers two functional surfaces for the attachment of different kinds of molecules, making such species especially attractive as multifunctional probes for diagnostic and therapeutic applications.[3] $Au–Fe_3O_4$ nanoparticles represent one such multifunctional system. They contain both Au and Fe_3O_4 nanoparticles, which are known to be biocompatible and have been used extensively for optical and magnetic applications in biomedicine.[4] Compared with conventional single-component Au or Fe_3O_4 nanoparticles, the dumbbell-like $Au–Fe_3O_4$ systems have distinct advantages: 1) The structure contains both a magnetic (Fe_3O_4) and an optically active plasmonic (Au) unit and is suitable for simultaneous optical and magnetic detection. 2) The presence of Fe_3O_4 and Au surfaces facilitates the attachment of different chemical functionalities for target-specific imaging and delivery applications. 3) The size of either of the two nanoparticles can be controlled to optimize magnetic and optical properties, and the small particle is only capable of accommodating a few DNA strands, proteins, antibodies, or therapeutic molecules, thus facilitating kinetic studies in cell targeting and drug release. Herein, we report that dumbbell $Au–Fe_3O_4$ nanoparticles can be made biocompatible and used as magnetic and optical probes for cell imaging applications.

Figure 1a illustrates the functionalized dumbbell-like 8–20-nm (core particle diameter) $Au–Fe_3O_4$ nanoparticles that were prepared and tested for this study. The dumbbell nanoparticles were first synthesized by decomposing iron pentacarbonyl on the surfaces of Au nanoparticles in the presence of oleic acid and oleylamine, as described previously.[1a] For control purposes, 8-nm Au, 20-nm Fe_3O_4, and 3–20-nm $Au–Fe_3O_4$ nanoparticles (see Figure S1 in the Supporting Information) were also prepared. The as-synthesized nanoparticles were coated with a layer of oleate and oleylamine and were further functionalized by a surfactant exchange reaction. The epidermal growth factor receptor antibody (EGFRA) was linked to the Fe_3O_4 surface through polyethylene glycol (PEG, $M_r = 3000$) and dopamine. The Au particle was protected with HS-PEG-NH_2 ($M_r = 2204$), with the thiol attaching to Au. The functionalized nanoparticles shown in Figure 1a were characterized by matrix-assisted laser desorption/ionization (MALDI) mass spectrometry (see Figure S2 in the Supporting Information). The antibody and two kinds of polyethylene glycol species can be successfully linked to the particles.

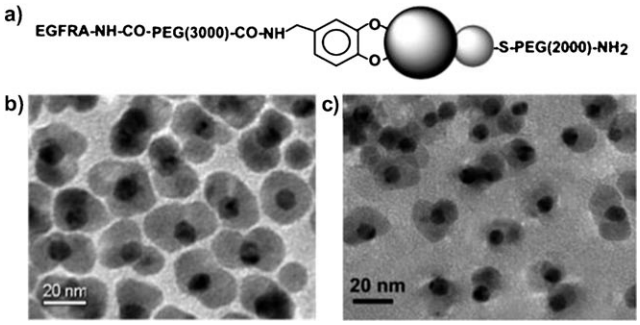

Figure 1. a) Schematic illustration of surface functionalization of the $Au–Fe_3O_4$ nanoparticles. b, c) TEM images of the 8–20-nm $Au–Fe_3O_4$ particles before (b) and after (c) surface modification.

These dumbbell nanoparticles were stable against aggregation in phosphate buffered saline (PBS) or PBS containing 10% fetal bovine serum (FBS) at 37°C for over 12 h, as evidenced by their unchanged hydrodynamic sizes (see

[*] C. Xu, J. Xie, C. Wang, Dr. N. Kohler, Prof. S. Sun
Department of Chemistry
Brown University
Providence, RI 02912 (USA)
Fax: (+1) 401-863-9046
E-mail: ssun@brown.edu
D. Ho, Prof. J. R. Morgan
Center for Biomedical Engineering
Brown University
Providence, RI 02912 (USA)
Prof. E. G. Walsh
Department of Neuroscience
Brown University
Providence, RI 02912 (USA)
Prof. Y. E. Chin
Department of Surgery, School of Medicine
Brown University
Providence, RI 02903 (USA)

[**] This work was supported by NIH 1R21CA12859-01, the Ittleson Foundation, the Dr. Ralph and Marian Falk Medical Research Trust, the Salomon award from Brown University, the Frontier Research Award from the Department of Chemistry, Brown University, and in part by NSF/DMR 0606264 and New England Regional Center of Excellence. We thank Dr. Takahiro Hiroi and KECK/NASA Reflectance Experiment Laboratory at Brown University for reflection spectrum measurement.

Supporting information for this article is available on the WWW under http://www.angewandte.org or from the author.

Figure S3 in the Supporting Information). Note that the size increase of the functionalized nanoparticles in PBS with 10% FBS is presumably due to the interaction between the negatively charged FBS and the antibody present on the surface of the particles. Transmission electron microscope (TEM) images of the dumbbell nanoparticles showed a slight size reduction in Fe_3O_4 after surface modification (Figure 1c). This effect is likely caused by the corrosion of Fe_3O_4 induced by dopamine during the surfactant exchange process.

Magnetic measurements show that the nanoparticles are superparamagnetic at room temperature before and after surface modification (Figure 2a). The nanoparticles also

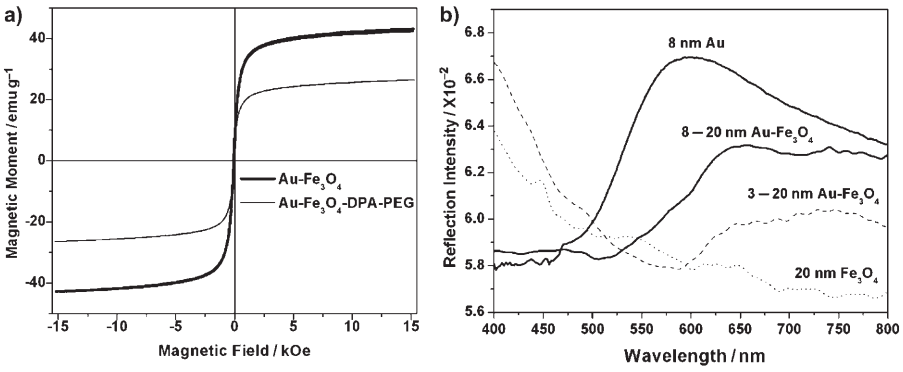

Figure 2. a) Magnetic hysteresis loops of the dumbbell nanoparticles before and after surface modification. The reduction of saturation magnetization is due largely to the weight contribution from the nonmagnetic Au particles. b) Reflection spectra of 20-nm Fe_3O_4, 8-nm Au, 3–20-nm Au–Fe_3O_4, and 8–20-nm Au–Fe_3O_4 nanoparticles.

fied Eagle's Medium (DMEM) containing 10% FBS for 1 h and subsequently washed the cells three times with PBS. The preferred binding between EGFR and EGFRA enabled the dumbbell nanoparticles to be populated on the surface or within the cytoplasm of A431 cells. Magnetic resonance imaging (MRI) analyses revealed that 20-nm Fe_3O_4 particles, the dumbbell nanoparticles, and A431 cells labeled with 8–20-nm Au–Fe_3O_4 nanoparticles shorten the T_2 relaxation of the water molecules, as shown in the MRI phantom images in Figure 3a. The iron content in all samples was determined by inductively coupled plasma atomic emission spectrometry (ICP-AES) and used for calculating relaxivities. Table 1 gives the relaxivity data on r_1, r_2, and r_2/r_1. The slight increase in r_1 and reduction in r_2 with the increase in size of the Au core seems to indicate a larger junction effect (reduced magnetization) in the dumbbell structure. Furthermore, 8–20-nm Au–Fe_3O_4 nanoparticles attached to A431 cells show smaller T_1 and T_2 relaxivities than the free nanoparticles. This behavior is similar to what has been observed in the iron oxide nanoparticle–monocyte system—cellular compartmentalization of the nanoparticles reduces proton relaxivity.[7] Detailed studies about this difference are underway.

exhibit a plasmonic absorption in PBS at 525 nm for 8-nm Au nanoparticles and at 530 nm for 8–20-nm Au–Fe_3O_4 dumbbell nanoparticles (see Figure S4 in the Supporting Information). The slight red shift is due to the junction effect in the dumbbell structure.[1a] More interestingly, self-assembled nanoparticle assemblies on an aluminum substrate coated with Teflon S (Boyd Coatings Research Co., Inc; the coating makes the reflection of the substrate less than 5%) exhibit characteristic reflectance in the 590–650-nm range. Figure 2b shows the reflectance spectra of the 8-nm Au and 20-nm Fe_3O_4 nanoparticles as well as the 3–20-nm and 8–20-nm Au–Fe_3O_4 dumbbell nanoparticles. The relatively weak reflectance from the dumbbell particles is likely caused by the dilution effect of Fe_3O_4 on Au in the dumbbell structure. For comparison, Fe_3O_4 nanoparticles have no reflectance in the same wavelength region. These magnetic and optical studies reveal that the dumbbell nanoparticles are both magnetically and optically active and can be used as dual functional probes for cell imaging applications. As an initial in vitro test, we demonstrate that the dumbbell nanoparticles are suitable as a probe for A431 (human epithelial carcinoma cell line) cell imaging.

A431 cells are known to overexpress EGFR and are commonly used to assess EGFRA therapy.[5] Imaging EGFR-overexpressed cells and tissues can potentially be used for early diagnostics and therapies of numerous cancers, including breast and lung cancers.[6] We incubated the EGFRA–dumbbell nanoparticles with A431 cells in Dulbecco's Modi-

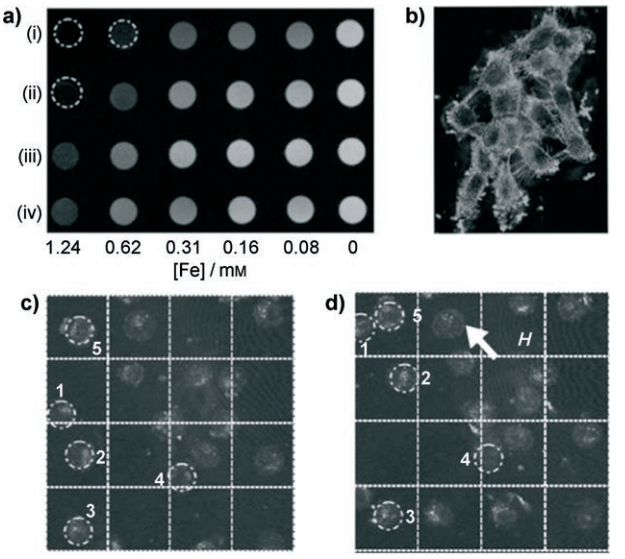

Figure 3. a) T_2-weighted MRI images of i) 20-nm Fe_3O_4, ii) 3–20-nm Au–Fe_3O_4, iii) 8–20-nm Au–Fe_3O_4 nanoparticles, and iv) A431 cells labeled with 8–20-nm Au–Fe_3O_4 nanoparticles. b) Reflection images of the A431 cells labeled with 8–20-nm Au–Fe_3O_4 nanoparticles. c, d) Images of A431 cells labeled with 8–20-nm dumbbell particles, floating in the medium before (c) and after (d) an external magnetic field was applied (field gradient in the sample area was in 500–100 G). The dashed circles denote individual cells; the numbers label the same cells in (c) and (d); the arrow and *H* indicate the direction of the applied magnetic field.

Table 1: Relaxivities r_1 and r_2 of Fe_3O_4 and Au–Fe_3O_4 nanoparticles with various Au core sizes for the same Fe_3O_4 size at 3 T ($T = 25°$).

Samples	r_1 [s^{-1} mM^{-1}]	r_2 [s^{-1} mM^{-1}]	r_2/r_1
Fe_3O_4	1.38	121.13	110.36
Fe_3O_4–Au (3 nm)	1.62	114.58	70.80
Fe_3O_4–Au (8 nm)	3.56	105	29.48
Fe_3O_4–Au (8 nm) in cell	2.17	80.4	37.1

A431 cells labeled with 8–20-nm Au–Fe_3O_4 nanoparticles were visualized with a scanning confocal microscope. The wavelength used for the image was 594 nm, which is close to the strong reflectance of the nanoparticles (Figure 3b). The signal detected from the dumbbell nanoparticles reflects the typical morphology of epithelial cells under the attachment conditions (1 μM Au and 8.8 μM Fe, Figure 3b) and is much stronger in the region of cell–cell contact, suggesting that EGFRA is involved in cell gap junction.[8] Furthermore, A431 cells labeled with the dumbbell nanoparticles can be manipulated by an external magnetic field, which is readily tracked under the optical microscope (Figure 3c,d).

The sample used for obtaining Figure 3b was re-imaged after three days and showed no signal loss (Figure 4a). This result is extremely important for long-term tracking of the

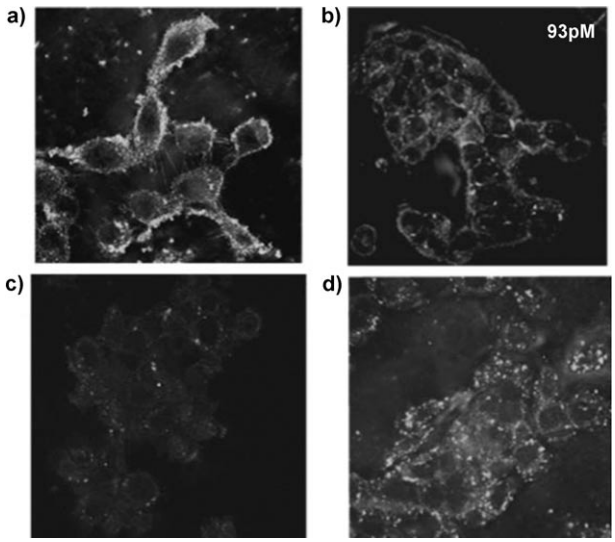

Figure 4. a) Reflection image of the labeled cells used to obtain Figure 3b after three days. b) Detection-limit examination of the 8–20-nm Au–Fe_3O_4–EGFRA labeled A431 cells. c) Reflection image of Fe_3O_4-labeled A431 cells. d) Reflection image of Au–Fe_3O_4 labeling without EGFR antibody.

nanoparticles in cellular structures. The detection limit for the 8–20-nm dumbbell is 90 pM Au (Figure 4b), which is 10^4 times lower than the normal detection concentration (Figure 3b or Figure 4a). In contrast, Fe_3O_4 nanoparticles yield much weaker reflectance signals (Figure 4c). To demonstrate the specific targeting, we incubated A431 cells and the 8–20-nm Au–Fe_3O_4 nanoparticles without EGFRA (Figure 4d) under the same concentration as that shown in Figure 4a. The reflection signal is much weaker, and the signal-to-noise ratio is much higher compared with Figure 4a, thus indicating that the EGFRA-labeled nanoparticles have higher specificity in their attachment to A431 cells. It is worth noting that the modified particles show negligible toxicity to A431 cells at 0.01 mg Fe mL^{-1} and 0.004 mg Au mL^{-1} (see Figure S5 in the Supporting Information).

The work presented herein demonstrates that through proper surface functionalization, the new dumbbell Au–Fe_3O_4 nanoparticles can be made biocompatible and suitable for linking different functional molecules to each end of the structure. The EGFRA-conjugated dumbbell nanoparticles show higher specificity in their attachment to A431 cells than those without EGFRA. The nanoparticles are magnetically and optically active and are therefore useful for simultaneous magnetic and optical detection. The fact that the dumbbell nanoparticles are capable of imaging the exact same tissue area through both MRI and an optical source without the fast signal loss observed in the common fluorescent labeling implies that they can be used to achieve high sensitivity in diagnostic imaging applications. Work on attaching therapeutic molecules to these dumbbell nanoparticles for target-specific imaging and delivery is under way.

Experimental Section

Reagents: α,ω-Bis{2-[(3-carboxy-1-oxopropyl)amino]ethyl}polyethylene glycol ($M_r = 3000$), *O*,*O*′-bis(2-aminoethyl)polyethylene glycol 2000, other chemicals, and organic solvents were purchased from Sigma Aldrich. *N*-Hydroxysuccinimide (NHS) and *N*,*N*′-dicyclohexylcarbodiimide (DCC) were from Pierce Biotechnology. All the buffers and media were from Invitrogen Corp. Water was purified by a Millipore Milli-DI Water Purification system. Nanosep 100k OMEGA was from Fisher. All the dialysis bags were purchased from Spectrum Laboratories, Inc. Epidermal growth factor receptor antibody was purchased from Santa Cruz Biotech Corp.

Instruments: Reflection spectra were acquired on a UV/Vis/NIR bidirectional spectrometer in the reflectance experiment laboratory (RELAB) of Brown University. The hysteresis loop was obtained at 300 K with a LakeShore 7400 VSM system. UV/Vis absorption spectra were obtained with a PerkinElmer Lambda 35 UV/Vis spectrometer. Mass spectrometry of the modified nanoparticles was performed on a matrix-assisted laser desorption ionization (MALDI) system. Optical images of A431 cells were obtained by a Zeiss Leica inverted epifluorescence/reflectance laser scanning confocal microscope. The TEM image was taken on a Philips EM 420 instrument (120 kV). The hydrodynamic diameters of the nanoparticles were measured using a Malvern Zeta Sizer Nano S-90 dynamic light scattering (DLS) instrument.

Synthesis of nanoparticles: Fe_3O_4 nanoparticles, Au nanoparticles, and Au–Fe_3O_4 nanoparticles were synthesized according to Yu et al.[1a]

Modification of nanoparticles: For modification of both Fe_3O_4 and Au–Fe_3O_4 particles, PEG diacid (20 mg), NHS (2 mg), DCC (3 mg), and dopamine hydrochloride (1.27 mg) were dissolved in a mixture of $CHCl_3$ (2 mL), DMF (1 mL), and anhydrous Na_2CO_3 (10 mg). The solution was stirred at room temperature for 2 h before nanoparticles (5 mg) were added, and the resulting solution was stirred overnight at room temperature under N_2. The modified nanoparticles were precipitated by adding hexane (5 mL), collected by a permanent magnet and dried under N_2. The particles were then dispersed in water or PBS. The extra surfactants and other salts were removed by dialysis using a dialysis bag (MWCO 10000) for 24 h in PBS or water. Any precipitate was removed by a 200-nm syringe filter (MillexGP). The final concentration of the particles was determined

by ICP-AES analysis. To link EGFR antibody and nanoparticles, a solution of nanoparticles (1 nmol) in PBS was mixed with 1-ethyl-3-(3-dimethylaminopropyl)carbodiimide (EDC; 1 μmol) for 15 min. After addition of EGFRA (4–5 nmol), the solution was rocked for 1 h and separated from the unattached antibody with Nanosep (PALL Life Science Corp.). For Au–Fe_3O_4 nanoparticles, HS-PEG-NH_2 was added after EGFRA was connected. After stirring for 3 h, the conjugates were subjected to dialysis to remove free HS-PEG-NH_2. The nanoparticles were analyzed by MS to confirm the modification.

Synthesis of HS-PEG-NH_2: 12-(Acetylthio)dodecanoic acid was prepared according to Xu et al.[9] The thiol-protected compound was then mixed with one equivalent *O*,*O*′-bis(2-aminoethyl)polyethylene glycol 2000 under EDC catalysis. Later, the protecting group was removed by reduction with hydrazine acetate. (MALDI MS: *m*/*z* 2204).

Cell experiments: A431 cells were purchased from ATCC and cultured in a glass-bottom Petri dish (MatTek Corp.) with Dulbecco's modified Eagle's medium (DMEM) with 10% FBS and 1% antibiotics. Before incubation with particles, the cells were washed with PBS three times. The particle solution in DMEM was incubated with cells for 1 h. Then, those cells were washed with PBS three times and fixed by 4% paraformaldehyde solution. After 30 min fixation, the cells were again washed three times with PBS and subjected to reflection imaging using a Leica TCS SP2 AOBS spectral confocal microscope.

Cell viability test: Viability of cells with particles was examined through WST1 assay.[10] This cell viability test is based on the cleavage of the tetrazolium salt WST-1 (4-[3-(4-iodophenyl)-2-(4-nitrophenyl)-2*H*-5-tetrazolio]-1,6-benzene disulfonate) by mitochondrial dehydrogenases in metabolically active cells. The cells were seeded onto 96-well culture plates at a density of 10^5 cells per well in DMEM (100 μL) containing 10% FBS. After 24 h incubation at 37 °C, nanoparticles in DMEM buffer at different concentrations were added. The particles were washed away after 48 h incubation. Then WST-1 solution (10 μL, Invitrogen) was added to each well to evaluate cell viability. After 4 h at 37 °C, cell viability was measured using a microplate reader.

MRI experiments: Transverse T_2-weighted spin echo images were acquired using a 3 T Siemens Tim Trio MR Scanner. Echo times were 11–132 ms in 11-ms steps with a repetition time of 2000 ms. T_1-weighted imaging was performed using inversion recovery with 10 inversion times ranging from 100 ms to 2000 ms with a repetition time of 3000 ms. Gel preparations in 2-mL vials were placed in a holder for insertion into the eight-channel volume head resonator. The long axis of the vials was parallel to the static magnetic field, and a transverse tomographic plane orientation was used. A gradient echo acquisition was used with a repetition time of 2000 ms, an echo time of 1.8 ms, a slice thickness of 12 mm, and a flip angle of 20°. In-plane resolution was 0.41 mm. The normal first-order shim process was applied, and the phantoms were imaged at room temperature (20 °C). For A431 cell experiments, 18000 A431 cells with attached dumbbell nanoparticles were mixed into 4% agarose gel at 40 °C before imaging.

Received: September 24, 2007
Published online: November 8, 2007

Keywords: antibodies · magnetic properties · magnetic resonance imaging · nanoparticles · reflection imaging

[1] a) H. Yu, M. Chen, P. M. Rice, S. X. Wang, R. L. White, S. H. Sun, *Nano Lett.* **2005**, *5*, 379–382; b) H. W. Gu, R. K. Zheng, X. X. Zhang, B. Xu, *J. Am. Chem. Soc.* **2004**, *126*, 5664–5665; c) T. Teranishi, Y. Inoue, M. Nakaya, Y. Oumi, T. Sano, *J. Am. Chem. Soc.* **2004**, *126*, 9914–9915; d) W. L. Shi, H. Zeng, Y. Sahoo, T. Y. Ohulchanskyy, Y. Ding, Z. L. Wang, M. Swihart, P. N. Prasad, *Nano Lett.* **2006**, *6*, 875–881; e) J. Yang, H. I. Elim, Q. B. Zhang, J. Y. Lee, W. Ji, *J. Am. Chem. Soc.* **2006**, *128*, 11921–11926; f) N. Glaser, D. J. Adams, A. Böker, G. Krausch, *Langmuir* **2006**, *22*, 5227–5229.

[2] a) A. Wood, M. Giersig, P. Mulvaney, *J. Phys. Chem. B* **2001**, *105*, 8810–8815; b) M. Haruta, *Gold Bull.* **2004**, *37*, 27–36; c) Y. Li, Q. Zhang, A. N. Nurmikko, S. H. Sun, *Nano Lett.* **2005**, *5*, 1689–1692.

[3] a) H. W. Gu, Z. M. Yang, J. H. Gao, C. K. Chang, B. Xu, *J. Am. Chem. Soc.* **2005**, *127*, 34–35; b) J. S. Choi, Y. W. Jun, S. I. Yeon, H. C. Kim, J. S. Shin, J. Cheon, *J. Am. Chem. Soc.* **2006**, *128*, 15982–15983.

[4] a) K. Sokolov, M. Follen, J. Aaron, I. Pavlova, A. Malpica, R. Lotan, R. Richards-Kortum, *Cancer Res.* **2003**, *63*, 1999–2004; b) D. A. Schultz, *Curr. Opin. Biotechnol.* **2003**, *14*, 13–22; c) Q. A. Pankhurst, J. Connolly, S. K. Jones, J. Dobson, *J. Phys. D* **2003**, *36*, R167–R181; d) I. H. El-Sayed, X. H. Huang, M. A. El-Sayed, *Nano Lett.* **2005**, *5*, 829–834; e) A. K. Gupta, R. R. Naregalkar, V. D. Vaidya, M. Gupta, *Nanomedicine* **2007**, *2*, 23–39.

[5] a) H. Haigler, J. F. Ash, S. J. Singer, S. Cohen, *Proc. Natl. Acad. Sci. USA* **1978**, *75*, 3317–3321; b) T. Kawamoto, J. D. Sato, A. Le, J. Polikoff, G. H. Sato, J. Mendelsohn, *Proc. Natl. Acad. Sci. USA* **1983**, *80*, 1337–1341.

[6] a) G. P. Adams, L. M. Weiner, *Nat. Biotechnol.* **2005**, *23*, 1147–1157; b) R. S. Herbst, *Int. J. Radiat. Oncol. Biol. Phys.* **2004**, *59*, S21–S26.

[7] G. H. Simon, J. Bauer, O. Saborovski, Y. J. Fu, C. Corot, M. F. Wendland, H. E. Daldrup-Link, *Eur. Radiol.* **2006**, *16*, 738–745.

[8] V. A. Krutovskikh, S. M. Troyanovsky, C. Piccoli, H. Tsuda, M. Asamoto, H. Yamasaki, *Oncogene* **2000**, *19*, 505–513.

[9] C. J. Xu, K. M. Xu, H. W. Gu, X. F. Zhong, Z. H. Guo, R. K. Zheng, X. X. Zhang, B. Xu, *J. Am. Chem. Soc.* **2004**, *126*, 3392–3393.

[10] M. Ishiyama, H. Tominaga, M. Shiga, K. Sasamoto, Y. Ohkura, K. Ueno, *Biol. Pharm. Bull.* **1996**, *19*, 1518–1520.

